

# Lyman-A Escape Fraction Corrections Approaches in Astro Stimulations

Haifeng Guo \*

Qingdao No.2 Middle School, Qingdao, 266000, China

\* Corresponding Author Email: ghfmine163@163.com

**Abstract.** The escape of Ly $\alpha$  photons from galaxies plays a critical role in understanding high-redshift star-forming galaxies (SFGs) and their contribution to cosmic reionization. This study examines the factors influencing the Ly $\alpha$  escape fraction ( $f_{esc}^{Ly\alpha}$ ), with a focus on the effects of dust, gas dynamics, and intergalactic medium (IGM) interactions. This work presents two methods for estimating Ly $\alpha$  escape, comparing them with existing observational data. The findings highlight the challenges in detecting Ly $\alpha$  emission in dusty galaxies and propose new techniques to account for the influence of dust attenuation and turbulent velocities on photon escape. By utilizing data from the THESAN cosmological simulations and considering local gas properties, this work develops a simple model of Ly $\alpha$  emission using extinction. By another independent stimulation statistic code, this work develop a more refined model incorporating corrections for local temperature, turbulent velocities, and dust absorption. The results suggest a better understanding of the relationship between dust, gas dynamics, and Ly $\alpha$  photon escape, with implications for studies of galaxy formation, star formation rates, and the impact of reionization. It provides direct correction with quantities including dust optical depth, temperature, hydrogen density and turbulent velocity. Further research will focus on refining this model with additional observations and complex gas kinematics.

**Keywords:** Lyman-alpha emission, escape fraction, Star forming observations, Lyman-alpha absorption.

## 1. Introduction

The Ly $\alpha$  line, while intrinsically very strong and therefore an attractive target for observations, undergoes a very complicated process escaping a galaxy due to the resonant nature of the line, as well as dust within the galaxies, inflows and outflows, and the intergalactic medium (IGM). Understanding the escape of these Ly $\alpha$  photons is of paramount importance to the characterisation of these high-redshift SFGs as well as to understanding their impact on extragalactic processes such as cosmic reionisation [1]. However, aside from the effects of redshift, the impact of the presence and motion of matter on Lyman-alpha is difficult to estimate, particularly because the microscopic physical processes in local regions are challenging to study. In this work, this work provides two methods to estimate, depending on the available observables, and comparing them with existing data.

For example, more recent multiwavelength observations of LAEs (Ly $\alpha$  emitters) in optical, infrared and submillimetre suggest that there are LAEs that are indeed old and dusty. The existence of a substantial amount of dust appears incompatible with strong Ly $\alpha$  emission. There must be a physical mechanism for Ly $\alpha$  photons to escape from such dusty galaxies.

The intrinsic Ly $\alpha$  luminosity of a galaxy is proportional to its SFR [2], and thus the intrinsically bright LAEs are hosted typically by massive haloes. However, such massive galaxies are also aged and dusty. Because of the strong dust absorption of Ly $\alpha$  photons, dusty star-forming galaxies do not appear as LAEs in the pure absorption model, there must be other factors that should be taken into consider [2].

Recently,  $f_{esc}^{Ly\alpha} = L_{Ly\alpha}/8.7 \times L_{H\alpha}$  is commonly adopted by researchers to try some new astronomical observations[3]. Ly $\alpha$  is the transition from  $n=2$  to  $n=1$  (wavelength 1216 Å). While H $\alpha$  is the transition from  $n=3$  to  $n=2$  (wavelength 6563 Å). It is based on an assumption that refers to a theoretical model where hydrogen is mostly in excited states, and the majority of the emission comes from these transitions. It assumes that Ly $\alpha$  photons are not scattered or reabsorbed, and thus, the

ratio between the Ly $\alpha$  and H $\alpha$  luminosities is a constant. However, there are some limitations of using the formula. This method assumes conditions and does not account for the possible dust absorption of Ly $\alpha$ , which can reduce the observed Ly $\alpha$  flux, especially in dustier galaxies. For galaxies with significant dust absorption, the Ly $\alpha$  escape fraction might be underestimated using this formula. The method is typically applicable to galaxies where the H $\alpha$  emission is less affected by dust, and Ly $\alpha$  photons are the primary tracer of the gas's ionized regions. Overall, with well corrected  $f_{\text{esc}}^{\text{Ly}\alpha}$ , potential dusty LAEs can be detected.

## 2. Corrections of Different Contributions from IGM & CGM

Many studies have investigated the contributions of different cosmic components, such as the IGM and CGM, to the Lyman-alpha luminosity; however, most of them rely on simplified empirical relations or adopt the same  $f_{\text{esc}}^{\text{Ly}\alpha}$  through different area. In the temperature range ( $10^4\text{K} - 10^5\text{K}$ ), free electrons possess sufficient kinetic energy to excite neutral hydrogen (HI) through collisions, resulting in efficient Ly $\alpha$  photon production. As the temperature increases beyond  $10^5\text{K}$ , most of the neutral hydrogen becomes ionized, reducing the availability of HI for excitation and thus decreasing the collisional Ly $\alpha$  emission. After corrections due to local gas qualities, this result might change.

### 2.1. THESAN Simulations Selections

The THESAN project was specifically designed to enable simultaneous exploration of cosmic reionization and galaxy formation with unprecedented detail. This goal is achieved by extending the IllustrisTNG galaxy formation framework with radiative transfer, non-equilibrium heating and cooling, physically motivated ionizing sources such as binary stars and active galactic nuclei, and a comprehensive model of dust formation, growth, and destruction. The simulations utilize the advanced Arepo-RT moving-mesh hydrodynamics code and were executed on some of the world's most powerful supercomputers. The suite includes a high-resolution flagship run that balances physical realism and simulated volume, resolving hundreds of thousands of galaxies across a region over 300 million light years in size. In addition, several medium-resolution simulations explore alternative physics models, numerical convergence, the relation between escape fraction and galaxy mass, as well as scenarios involving different dark matter models. as shown in Figure 1.

Name	SED	Filaments	catalogs				
			Groups	Ly $\alpha$	Cross-match	LOS	$f_{\text{esc}}$
THESAN-1	✓	✓	✓	✓	✓	✓	✓
THESAN-2	✗	✓	✓	✓	✓	✓	✓
THESAN-WC-2	✗	✓	✓	✓	✓	✓	✓
THESAN-HIGH-2	✗	✓	✓	✓	✓	✓	✓
THESAN-LOW-2	✗	✓	✓	✓	✓	✓	✓
THESAN-SDAO-2	✗	✓	✓	✓	✓	✓	✓

**Fig. 1** THESAN Simulation types [4].

All accessible data is listed (with Ly $\alpha$ ), this work requires Cartesian result of snapshots, and this work finally chose HIGH-2 due to its accuracy.

### 2.2. UV Slope

The UV slope (commonly denoted as  $\beta$ ) describes the shape of a galaxy's ultraviolet (UV) continuum spectrum, usually over the wavelength range 1200–3000Å. It is often approximated by a power law:  $f_{\lambda} \propto \lambda^{\beta}$ . Hence this work can estimate  $\beta$  as 2 or more Luminosity at different wavelength are given,  $\beta = \log_{10}(L_{1500}/L_{2500})/\log_{10}(1500/2500)$ . The UV slope  $\beta$  is a reliable dust attenuation indicator only for young, starburst galaxies over the rest-frame 1250–2600Å range, and its interpretation becomes uncertain in older stellar populations, AGN, heavily dust-obscured systems, or at high redshift where Ly $\alpha$  forest absorption affects the spectrum.

## 2.3. Extinction

By empirical formula  $A_{1600} \approx 4.43 + 1.99\beta$ , and further given color excess  $E(B - V) = A_{1600}/k(1600)$  [5]. And in this part, it treats  $k$  as 10.0 for SMC dust. This work uses Semi-Analytic Model, SAM empirical formula

$$f_{\text{esc}}^{\text{Ly}\alpha} = C \times 10^{-0.4E(B-V)k(\text{Ly}\alpha)} \quad C = 0.22 \quad k(\text{Ly}\alpha) = 12.0 \quad (1)$$

However, the scatter around the relation is large, indicating strong dependence on gas geometry, HI column density, and kinematics [6]. Even in the absence of dust, the maximum escape fraction is only about 20%, due to resonant scattering increasing the effective path length. With an SMC-like extinction curve (steeper), the functional form is similar, but the best-fit normalization constant  $C$  changes.

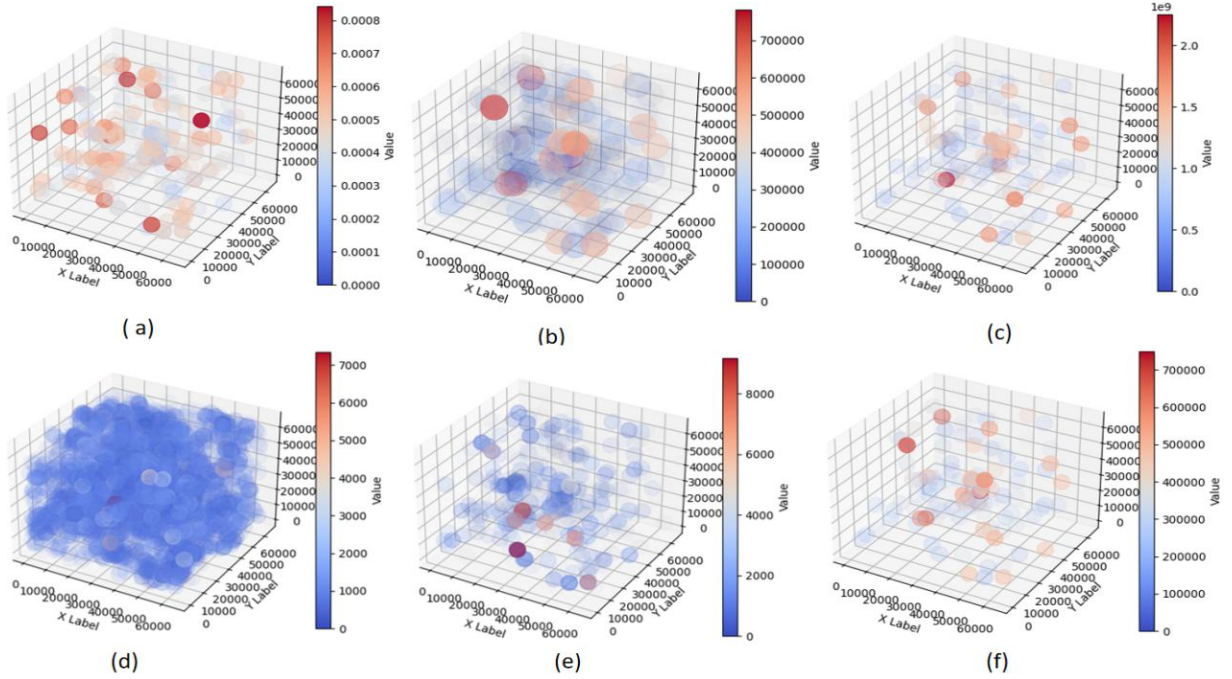


**Fig. 2** (b) and (f) are spatial Luminosity distribution for  $\lambda = 1216\text{\AA}$  (different spot size), (d) and (e) are spatial Luminosity distribution for  $\lambda = 1500\text{\AA}$  and  $\lambda = 2500\text{\AA}$ . (a) is spatial Luminosity distribution for escape fraction, (c) is theoretical (before absorbed) spatial Luminosity distribution for  $\lambda = 1216\text{\AA}$ . The smaller values are set into the more transparent point. (Picture credit: original)

From Fig.2 (a), it is found that spatial distribution of  $f_{\text{esc}}$  varies significantly by this method, although there is some systematic errors, such as redshift leading to small  $f_{\text{esc}}$ , it is proportionally correct. So compare (b) and (c), the position of the maximum observable LAE (Ly $\alpha$  emitter) has changed. While the dark areas with low Ly $\alpha$  luminosity are still at original position. Therefore, before absorption of dust, the potential Ly $\alpha$  Luminosity source has not been found, and CGM and IGM may cause different consequence to Ly $\alpha$ .

## 3. Self Stimulation Based on Abundant Variables

### 3.1. Crucial Variables: Dust Densities and Turbulent Velocity

The most robust approach is modeling infrared/sub-millimeter dust emission using observations from instruments such as Herschel or ALMA, typically with modified blackbody or Draine & Li dust models [7].

The most reliable method is spectral line width decomposition of HI 21 cm or CO molecular lines, separating thermal and instrumental broadening from the total linewidth to isolate the turbulent component [8]. Data in THESAN program is limited, to get real model of Ly $\alpha$  emission, further

quantities (local temperature, turbulent velocity, density of hydrogen, radical depth of dust) are needed.

### 3.2. Physic Process

In the python program, these physical processes are taken into consider thermal broadening (Maxwell distribution), line broadening by turbulent flow, Doppler shift, Dust absorption, Random Optical 1 Depth Sampling. By randomly generated particles, each goes through stimulated environment and being absorbed, sum the rest particles out of space, and gives a ratio. 1. Thermal broadening: The thermal velocity distribution of atoms follows the Maxwell Boltzmann distribution, with one-dimensional thermal velocity dispersion.

$$\sigma_{th} = \sqrt{\frac{k_B T}{m_H}} \quad \Delta v_{th} = \frac{v_0}{c} \sigma_{th} \quad (2)$$

So extra velocity is added to particles related to their temperature. 2. Turbulent Broadening:  $\sigma_{total} = \sqrt{\sigma_{th}^2 + \sigma_{turb}^2}$  so extra velocity is added to particles related to the randomly selected turbulent velocity. 3. Doppler shift:  $v' = v(1 - v_0/c)$  by setting  $V_0$ , it can affect whether photons approach resonance 4. Dust absorption:  $P_{survive} = \exp(-\tau_{dust})$  It is key to determine whether the particle disappears after scattering, to ensure light travels randomly in space.

### 3.3. Line of the Best Fit

This work inherits the empirical formula pattern from the previous section. Two steps of fit is used, Coarse fit and Fine fit (specially GPU acceleration used. For coarse fit, this work define a coarse parameter grid,  $\alpha \in [0.1, 2]$  (step 0.2),  $\beta \in [-1, 1]$  (step 0.2),  $v_b \in [10, 500]$  km/s (step 50). For each grid point, compute the model escape function:

$$f_{model}(n_H, T, v_{bulk}, \tau_{dust}) = \exp \left[ -a \frac{n_H^\alpha T^\beta}{1 + v_{bulk}/v_0} - b \tau_{dust} \right] \times T_{IGM} \quad (3)$$

and evaluate its discrepancy with the physical simulation result  $f_{sim}$

$$\chi^2 = \sum (\ln f_{model} - \ln f_{sim})^2 \quad (4)$$

Select the grid point with the minimum error and the initial guess

For Fine Fit, This work aim to refine the parameters within the promising region found in the coarse fit, to obtain the precise  $(a, \beta, V_0)$ . Several important procedures are listed below. Firstly, use the coarse fit solution as the starting point. Then this work performs nonlinear least squares optimization (Levenberg-Marquardt or Trust Region algorithms). Finally, this work iterates until convergence, yielding the final fitted parameters. Under fine fit, this work can achieve high accuracy while avoiding local minima problems because the coarse fit provides a good initialization.

In the first round, this work does several times of simulation, and final 5 times are given by Fig. 3. And This work optimum the codes to improve its accuracy and efficiency.

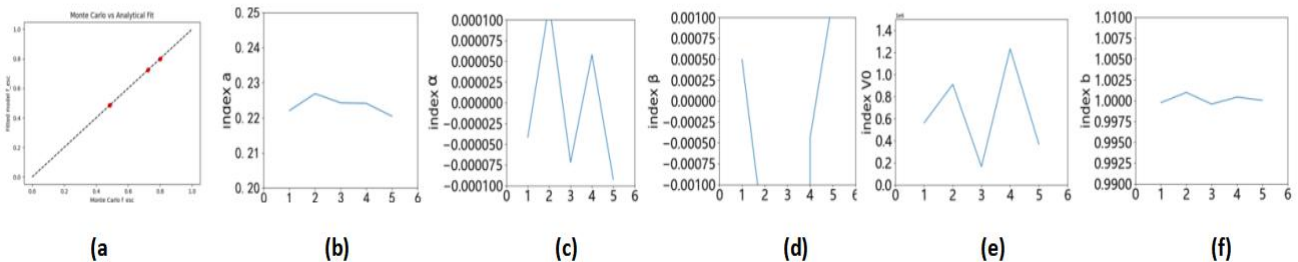


**Fig. 3** First run of stimulation. (a) is the target line and sapling distribution. (b)(c)(d)(e)(f) are final 5 times value of index a,  $\alpha$ ,  $\beta$ ,  $v_0$ , b (Picture credit: original).

Hence, only a and b are at acceptable error ranges, this work take  $b = 2.24$   $a = 1$  for later simulation. After these two variables were determined, this work conducted a second round of simulations with higher accuracy.

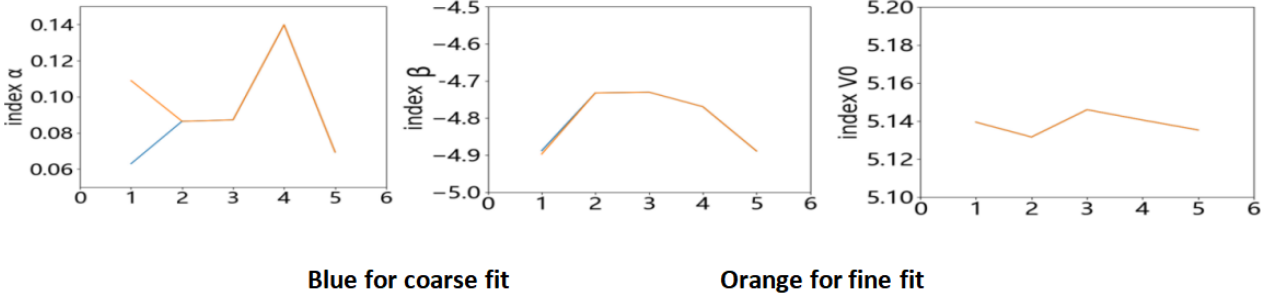


**Fig. 4:** Result for final 5 rounds simulations. Except  $\alpha$  is changing with 0.5 percentage uncertainty,  $\beta$  and  $V0$  is with 0.02 and 0.002 percentage uncertainties. (Picture credit: original)

### 3.4. Result

For fine fit, scale of alpha can be determined, beta can be determined, and  $V0$  can be determined. This work takes  $\text{Alpha} = 0.1$  (only correct in scale),  $\text{Beta} = -4.8$ ,  $V0 = 5.14$  (Fig.4), for subsequent research.

$$f_{\text{esc}}(n_{\text{H}}, T, v_{\text{bulk}}, \tau_{\text{dust}}) = \exp \left[ -\frac{n_{\text{H}}^{0.1} T^{-4.8}}{1 + v_{\text{bulk}}/5.14} - 2.24 \tau_{\text{dust}} \right] \times T_{\text{IGM}} \quad (5)$$

In the final result,  $T_{\text{IGM}}$  is a coefficient related to redshift and the neutral hydrogen fraction, this work take it as a constant 0.8.  $v_{\text{bulk}}$  is the turbulent velocity, its unit is kilometers per second.  $n_{\text{H}}$  is the density of total hydrogen, its unit is per cube centimeters.  $\tau_{\text{dust}}$  is optical depth, it is a dimensionless quantity. The result shows as expected to some relations.

### 3.5. Sample Scale

In the first round of simulations, only one pack of photons is used at certain times, increasingly from  $1e5$  to  $1e8$ . At the scale of  $1e8$ , two of five indexes are stable. In the second round of simulations, 200 packs of 10000 photons are included at each time of simulation. For the final 5 times of stimulation, this work increases to 1000 packs of 10000 photons, and the NumPy. Random Seeds in python are changed at every time of stimulation, ensuring all kinds of value arrangements are considered. Besides, every particle is formed with Temperature intervals  $1e4$  to  $2e5$ ,  $\tau_{\text{dust}}$  intervals from 0 to 1,  $v_{\text{bulk}}$  from 0 to 300,  $n_{\text{H}}$  from  $1e-4$  to  $1e4$ .

## 4. Discussion

### 4.1. Methods to Estimate Optical Depth and Hydrogen

The most influential variable in the formula is the  $\tau_{\text{dust}}$ , as the value of  $2.24 \tau_{\text{dust}}$  is always times magnitudes of the left part of the index, so accurate  $\tau_{\text{dust}}$  is crucial to accurate  $f_{\text{esc}}$ . In recent simulations, SED (Spectral Energy Distribution) is a reliable model to estimate  $\tau_{\text{dust}}$ . This work can construct a dust-free intrinsic SED using: Stellar population synthesis model that include stellar age, metallicity, and star formation history (SFH). AGN/galaxy templates built from observed samples. Compare the model SED with the observed one. The differences arise from: Dust attenuation curves. Redshift and flux normalization [9]. An example to access to more reliable  $\tau_{\text{dust}}$  is given by [9], In a clumpy ISM,  $\text{Ly}\alpha$  photons are scattered mostly at the surface of cold clumps before they are absorbed by dust. A large fraction of  $\text{Ly}\alpha$  photons can then escape from a clumpy ISM through multiple scatters. They use the number of subhalos of the galaxy as a measure of its 'clumpiness'. They introduce the clumpiness factor  $S$ , which depends on number of subhalos [10].

## 4.2. Data Analysis and Tradition Measurements

To better estimate the accuracy of the formula, this work does test real samples. HXMM01 galaxy, has Representative redshift, and lies at  $z = 2.3$ . It serves as a highly representative laboratory for studying galaxies under extreme conditions at high redshift. Besides, it has extreme star formation efficiency. HXMM01 is a merger of two massive galaxies, triggering intense starburst activity with a star formation rate exceeding 2000 solar masses per year, far above that of normal galaxies. It also has high dust temperatures and dense gas, strong turbulence and complex dynamics. The CO line width is several hundred km/s, corresponding to a turbulent velocity of about 100 km/s. Such strong turbulence provides a natural testbed for turbulence-related theoretical models. Meanwhile, as an extremely luminous infrared galaxy, HXMM01 absorbs nearly all its UV radiation and re-emits it in the infrared. This makes it a perfect case to study radiative transfer, optical depth, and escape fractions in dusty starbursts.

This work set  $n_H = 10000$ ,  $T = 55\text{K}$ ,  $v_{\text{bulk}} = 100\text{km/s}$ ,  $\tau_{\text{dust}} = 1$ , for corresponding calculations, as a result its  $f_{\text{esc}}^{\text{Ly}\alpha}$  is 0.085, which is reliable. And several examples show that lower bound of  $\tau_{\text{dust}}$  is a more practical choice in the formula.

## 4.3. $f_{\text{esc}}$ Change by Redshift

This work does not take redshift into consideration at all, instead of focusing on local micro physic process rather than global trends. However, Hayes has found that a gentle evolution over their redshift ranges that could be fitted with a power law of the form  $f_{\text{esc}} = C(1 + z)^\xi$ , where  $C = 4.79 \times 10^4$  and  $\xi = 3.38$  at  $z = 2.2-6.7$  [11]. In this stimulation, This work constantly treat  $T_{\text{IGM}} = 0.8$ , which might change significantly through universe evolution.

## 4.4. Further Research

This work wants to try to check the formula by some appropriate galaxies and astronomic systems and use the verified formula to distinguish small differences between LAEs, especially with more datasets from telescopes. Besides, this work did not consider more complex gas kinematics, including multi-phase gas flows, feedback from star formation, and the influence of active galactic nuclei (AGN), could impact the Ly $\alpha$  escape fraction. Further simulations incorporating these complex dynamics could lead to a more comprehensive understanding of Ly $\alpha$  emission in both star-forming galaxies and AGN-hosted galaxies. In addition, the current model adopts an empirical dust extinction law (SMC-like dust model) for simplicity. However, dust properties can vary significantly across different galaxy types and environments. Further work is required to model the varying dust attenuation curves in more detail, particularly in galaxies with mixed metallicities or unique star formation histories. A deeper understanding of the interplay between dust and Ly $\alpha$  emission will be crucial for accurately modeling  $f_{\text{esc}}$  and the impact of dust on the reionization process.

## 5. Conclusion

In this study, this work investigated the complex physical processes governing the escape of Lyman- $\alpha$  photons from galaxies, with particular emphasis on the roles of dust attenuation, turbulent velocities, and IGM/CGM medium interactions. By combining insights from the THESAN cosmological simulations with independent statistical modeling, this work developed a correction framework that incorporates key local variables, including dust optical depth, gas temperature, hydrogen density, and turbulent velocity. The results demonstrate that traditional approaches often underestimate the escape fraction in dusty or dynamically complex systems, while the refined model provides a more accurate description of Lyman- $\alpha$  emission across different environments.

These findings highlight the critical interplay between micro-scale processes (such as scattering and absorption) and macro-scale galactic dynamics in shaping observed Lyman- $\alpha$  properties. Moreover, the proposed correction model offers a practical tool for interpreting current and upcoming

observational datasets, thereby improving the understanding of high-redshift star-forming galaxies and their contribution to cosmic reionization. Future work should aim to extend this framework by incorporating more realistic gas kinematics, variable dust extinction laws, and comparisons with larger observational samples, ultimately leading to a more comprehensive picture of galaxy evolution in the early universe.

## References

- [1] Goovaerts I, Thai T T, Pello R, et al. Charting the Lyman- $\alpha$  escape fraction in the range  $2.9 < z < 6.7$  and consequences for the LAE reionisation contribution. *Astronomy & Astrophysics*, 2024, 690: A302.
- [2] Calzetti D. The dust extinction law in starburst galaxies. *The Astrophysical Journal*, 1997, 476(2):561-577.
- [3] Shimizu I, Yoshida N, Okamoto T. Lyman  $\alpha$  emitters in cosmological simulations–I. Lyman  $\alpha$  escape fraction and statistical properties at  $z = 3.1$ . *Monthly Notices of the Royal Astronomical Society*, 2011, 418(4): 2273-2282.
- [4] THESAN Simulation <https://thesan-project.com/thesan/index.html>
- [5] Henry A, Scarlata C, Martin C L, et al. Ly $\alpha$  emission from Green Peas: the role of circumgalactic gas density, covering, and kinematics. *The Astrophysical Journal*, 2015, 809(1): 19.
- [6] Calzetti, D., Armus, L., Bohlin, R. C., Kinney, A. L., Koornneef, J., & Storck-Bergmann, T. The Dust Content and Opacity of Actively Star-forming Galaxies. *The Astrophysical Journal*, 2000, 533: 682–695.
- [7] Draine B T, Li A. Infrared emission from interstellar dust. IV. The silicate-graphite-PAH model in the post-Spitzer era. *The Astrophysical Journal*, 2007, 657(2): 810.
- [8] Hayes M, Schaerer D, Östlin G, et al. On the redshift evolution of the Ly $\alpha$  escape fraction and the dust content of galaxies. *The Astrophysical Journal*, 2011, 730(1): 8.
- [9] Tielens A G G M. *The physics and chemistry of the interstellar medium*[M]. Cambridge University Press, 2005.
- [10] Hayes. Dust Absorption and the Ultraviolet Luminosity Density at  $z \approx 3$  as Calibrated by Local Starburst Galaxies *The Astrophysical Journal*, 2011, 521:64–80.
- [11] Walcher J, Groves B, Budavári T, et al. Fitting the integrated spectral energy distributions of galaxies. *Astrophysics and Space Science*, 2011, 331(1): 1-51.